ECS Transactions, 64 (47) 25-32 (2015)
10.1149/06447.0025ecst ©The Electrochemical Society

Boron-Doped Nanocrystalline Diamond Grown on Reticulated Vitreous Carbon: Morphological, Structural, and Electrochemical Characterizations

S. S. Oishi[a], E. C. Botelho[b], M. C. Rezende[c], C. A. A. Cairo[d], M. R. Baldan[a], and N. G. Ferreira[a]

[a] LAS, Instituto Nacional de Pesquisas Espaciais, São José dos Campos, São Paulo 12227-010, Brazil
[b] Department of Materials and Technology, UNESP-Univ. Estadual Paulista, Guaratinguetá, São Paulo 12516-410, Brazil
[c] Institute of Science and Technology, UNIFESP-Univ. Federal de São Paulo, São José dos Campos, São Paulo 12231-280, Brazil
[d] Materials Division/ Institute of Aeronautics and Space, AMR/IAE/DCTA - São José dos Campos, São Paulo 12228-904, Brazil

Composites formed from diamond grown on carbonaceous materials have been showed special attention due to their remarkable properties for electrochemical applications. In this sense, boron-doped nanocrystalline diamond (BDND) films were grown on reticulated vitreous carbon (RVC) substrates produced from poly(furfuryl alcohol) at two heat treatment temperatures (HTT) of 1000 °C and 1700 °C. The films were produced from hot filament chemical vapor deposition reactor with an *in-situ* doping process in the gas phase. Scanning electron microscopy and Raman spectroscopy analyses confirmed that both RVC electrodes were totally covered by good quality nanodiamond coatings with acceptor concentrations at around 10^{20} B.cm^{-3}, evaluated by Mott-Shottky measurements. Both RVC/BDND composites presented good electrochemical response in redox couple. Nonetheless, RVC/BDND1700 showed the best conductivity due to its lowest variation of ΔE_p value as well as its highest electrochemical area. These results demonstrate that RVC/BDND1700 is a very promising electrode material.

Introduction

Vitreous carbon has been widely used as electrode since other materials do not have a balanced set of properties, such as light-weight, electric/thermal conductivity, corrosion resistance and low cost. Reticulated vitreous carbon (RVC) has been used as an electrode, particularly, to provide many accessible pores, facilitate high current densities, low electrical/fluid flow resistance and to hold impregnated materials within controlled pore sizes (1-3). According to the literature, RVC has a free void volume between 90% and 97%, depending on the ppi grade, and a surface area of around 65 cm^2 cm^{-3}, for the 100 ppi grade. This material does not combust after heating to bright incandescence in air followed by removal of the heat source. However, when heating above 315 °C in air can be generated significant oxidation, resulting in a material with enhanced adsorption

properties. It is highly resistant to intercalation by materials that disintegrate graphite and it is inert to a wide range of very reactive acids, bases, and organic solvents (4).

Microcrystalline diamond films electrodes doped with boron, nitrogen, metals and metallic groups have been extensively used due to their higher electrochemical performance compared to the vitreous carbon itself, graphite and platinum. Currently, studies on nano and ultrananodiamond started to be more explored since they have been highlighted because of their excellent electrical, mechanical, thermal and biocompatible properties (5-7).

In this work, RVC was processed impregnating polyurethane foams with poly(furfuryl alcohol) (PFA) resin and heat treated under a controlled atmosphere, resulting in a highly disordered non-crystalline structure. RVC microstructure or its graphitization index may be controlled by heat treatment temperature (HTT). As the HTT increases, RVC disorder decreases due mainly to the increase of its graphitization level (8,9). For electrochemical applications diamond growth on RVC substrates may produce a particular composite with good electrical conductivity depend on the RVC HTT as well as the diamond doping process.

In this sense, the mechanisms of diamond growth on RVC with different HTT have been already discussed (9,10). However, boron-doped nanodiamond growth (BDND) and electrochemical performance of RVC/BDND composites were not investigated. Therefore, the main purpose of this work is the production and characterization of BDND electrodes grown on RVC (RVC/BDND) by using Scanning Electron Microscopy (SEM), Raman spectroscopy, X-ray diffraction and Cyclic Voltammetry techniques. It was also discussed HTT influence on substrate structural properties related with diamond film growth and its electrochemical response.

Experimental

Reticulated vitreous carbon processing

RVC was processed using poly(furfuryl alcohol) resin synthesized according to the best condition established previously (11), except for the viscosity that was higher than specified in order to get a good resin anchorage. The resin had as main features: a viscosity of 21 Pa.s, pH around 3 and moisture of 2%. Polyurethane foams with 70 ppi (pores per inch) were used as matrix for the anchorage of PFA. Polyurethane foams were impregnated with PFA catalyzed with 3% of p-toluenosulfonic acid (60 w/v%) and cured in an oven for 1h in the following step heating: 50 °C, 70 °C, 90 °C, 110 °C and 130 °C.

The cured material was heat treated in a tube furnace, from room temperature until 1000 °C, remaining 1h at the final temperature, with a heating rate of 1 °C/min and inert atmosphere of nitrogen. For the samples heat treated at 1700 °C, a high temperature furnace was used with a heating rate of 5 °C/min and inert atmosphere of nitrogen. After HTT the material was cut in disk shape with 20 mm diameter.

Boron-Doped Nanocrystalline Diamond films growth

RVC samples were first prepared using seeding pretreatment to improve the diamond growth process. The substrates were immersed in a solution containing 0.25 µm of diamond particles dispersed in hexane solvent, followed by ultrasonic agitation for 2 h.

This substrate pretreatment is necessary in order to keep the surface carbon in sp^3 configuration dominant over sp^2 bond etching.

Nanocrystalline diamond films were grown by hot filament chemical vapor deposition (HFCVD) technique, using 5 filaments of tungsten with 125 µm diameter, placed at 6 mm of sample top and 18 h deposition time. Reactor pressure and the substrate temperature were kept at 4 kPa and 670 °C, respectively, with a gas mixture composed by 70.8% Ar, 28.3% H_2 and 0.88% CH_4. The boron doping was performed by additional hydrogen line passing through a bubbler containing B_2O_3 dissolved in CH_3OH. When B_2O_3 is dissolved in CH_3OH, trimethylborate ($B(CH_3O)_3$) is produced, which is probably the substance containing boron that is added to the gas mixture during the growth process. The solution was prepared with a concentration of B_2O_3 dissolved in CH_3OH that correspond to B/C ratio of 30,000 ppm.

Characterization

The morphology of RVC/BDND composites was evaluated by Scanning Electron Microscopy (SEM) using a JEOL-JSM-5310 model. The quality of the films was evaluated with micro-Raman scattering spectroscopy (Renishaw microscope system 2000) using 514.5 nm line of an argon ion laser. The X-ray diffraction patterns were used to investigate the BDND crystallinity using a PANanalytical model X'Pert Pro MPD diffractometer with the CuKα radiation (λ = 1.54 Å) using θ-2θ scan from 5° to 100°. Finally, the electrochemical behavior of the composites was studied by cyclic voltammetry measurements using an Autolab 302 equipment. A platinum coil wire served as the counter electrode and Ag/AgCl was used as the reference electrode. The voltammetric curves were taken in H_2SO_4 0.5 $mol.L^{-1}$. The electrochemical kinetic was applied by using the redox couple of $Fe(CN)_6^{3-/4-}$ with different scan rates in 0.5 $mol.L^{-1}$ H_2SO_4 + 1.0 $mmol.L^{-1}$ $K_4Fe(CN)_6$ solution.

Results and Discussion

Boron-doped nanodiamond films, grown on RVC produced at different temperatures, were firstly investigated by SEM. The nomenclatures of the two composites were formed according to the HTT of RVC (RVC/BDND 1000 and RVC/BDND 1700). According to the SEM images (Figure 1), the BDND film presents characteristic ballas morphology and not defined facets. RVC/BDND 1000 (Figure 1a) shows an uniform texture while RVC/BDND 1700 present some clusters of different sizes that were probably caused due to its high secondary nucleation process. The inset shows an image for each composite with lower magnification (200x) to show the BDND film recovering all the RVC stems.

According to previous works (9,12), films grown at higher HTT carbon substrate present a high nucleation rate since the carbon structure is more resistant to the hydrogen etching. Although RVC1000 presents a higher oxygen content which promotes OH formation that is more efficient to etching sp^2 and sp^3 bonds than atomic hydrogen itself, no carbon etching was observed on RVC/BDND 1000.

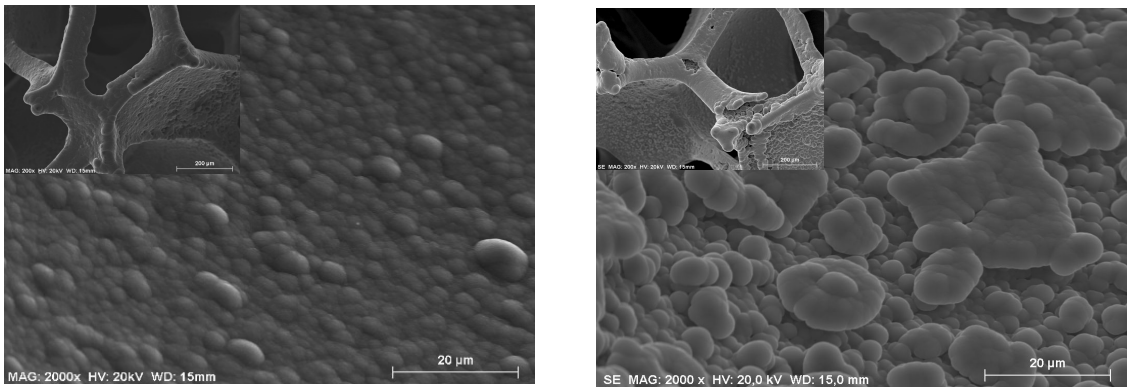

(a) (b)

Figure 1. SEM images of composites: (a) RVC/BDND 1000 and (b) RVC/BDND 1700.

Figure 2 shows the Raman spectra of the two RVC/BDND composites that confirm the morphology observed by SEM. Both spectra are similar and present a diamond peak at 1320 cm^{-1} overlapped by the D band at 1350 cm^{-1}. This down-shifting compared to the microcrystalline diamond peak is related to impurities formed in heavily doped films (13). The bands at 1150 and 1490 cm^{-1} can be related to the transpolyacetylene segments at the grain boundaries of the nanocrystalline diamond surface. More recently, Mortet et al. (14) argue that these bands have to be reassigned to a deformation mode of CH_x bonds, since this substance decompose at temperatures far below the deposition temperatures used in most CVD diamond experiments (around 700-900 °C). The band at 1550 cm^{-1} can be assigned to G band. The bands at 500 and 1220 cm^{-1}, related to the boron doping, are present in all spectra and are more evident for microcrystalline diamond films. The presence of the band at 500 cm^{-1} is attributed to the concentration increase in the boron pairs that have local vibration modes producing this wide band in this region that varies with the amount of boron incorporation (15).

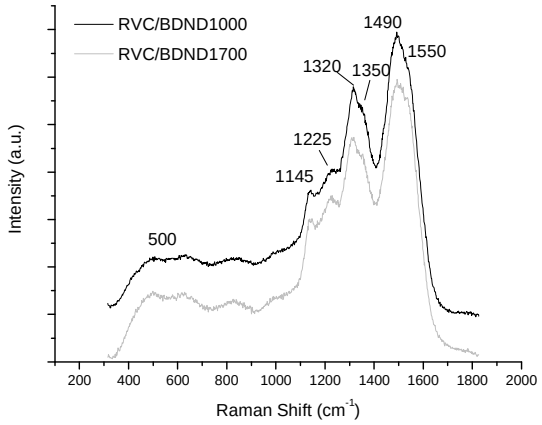

Figure 2. Raman spectra of RVC/BDND composites.

The XRD patterns of RVC/BDND1000 and RVC/BDND1700 are presented in Figure 3. In both patterns, the diamond peaks at 2θ = 44.0, 75.4 and 91.4° can be identified as the (111), (220) and (311) reflections of diamond. The carbon band (002) becomes sharper by increasing the HTT and also leading to the appearance of (004) band as a shoulder at 53.0°. The carbon band (100) appear overlapped by the (111) diamond peak. The average crystallite size can be calculated from the FWHM of (111) diffraction peak using the Scherrer law. The grain sizes obtained are 6.6 nm and 7.6 nm for RVC/BDND1000 and RVC/BDND1700, respectively. The lower grain size of RVC/BDND1000 can be related to the presence of oxygen that is responsible for changing the mechanism of diamond growth as already discussed previously (12).

The intensity ratio I_{220}/I_{111} shows the preferential growth in a polycrystalline film. For randomly oriented diamond powders this ratio is 0.25 (16). The ratios I_{220}/I_{111} calculated for RVC/BDND1000 and RVC/BDND1700 are 0.17 and 0.12, respectively. This result shows the films are dominated by a (111) texture and the lowest value for the film grown on RVC1700 is coherent with its highest grain size.

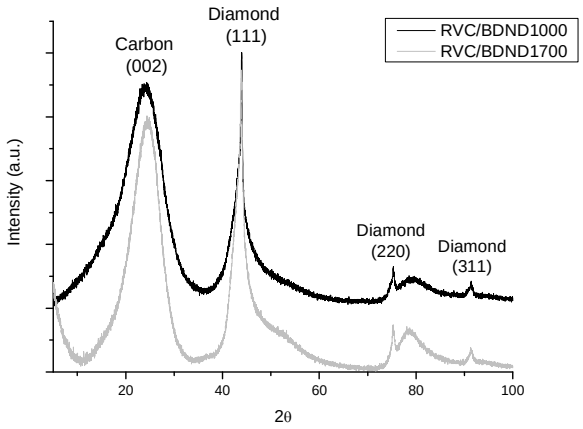

Figure 3. XRD patterns of RVC/BDND composites.

Figure 4a shows the working potential window in 0.5 mol L^{-1} H_2SO_4 solution for the RVC substrates as well as for RVC/BDND composites. RVC1000 electrode presents higher contribution of capacitive current probably associated to the presence of oxygen containing functional groups on its surface. Figure 4b shows cyclic voltammetry i-E curves using the redox couple $Fe(CN)_6^{3-/4-}$ with scan rate (v) of 50 mV s^{-1} for RVC and RVC/BDND heat treated at 1000 and 1700 °C. This redox system includes reactions that depend on the specific interactions with the surface functionalities on sp^2-bonded carbon electrodes. The results may be analyzed by the quasi-reversibility criteria: the separation between the anodic and cathodic peaks (ΔE_p) is larger than 59/n mV (where n=1 is the number of electrons involved in the reaction) and increases with v increase; current peak intensity (Ip) increases with $v^{1/2}$ increase, but does not keep proportionality; and the cathodic peak potential (E_{pc}) shifts to negative values, with v increase (17).

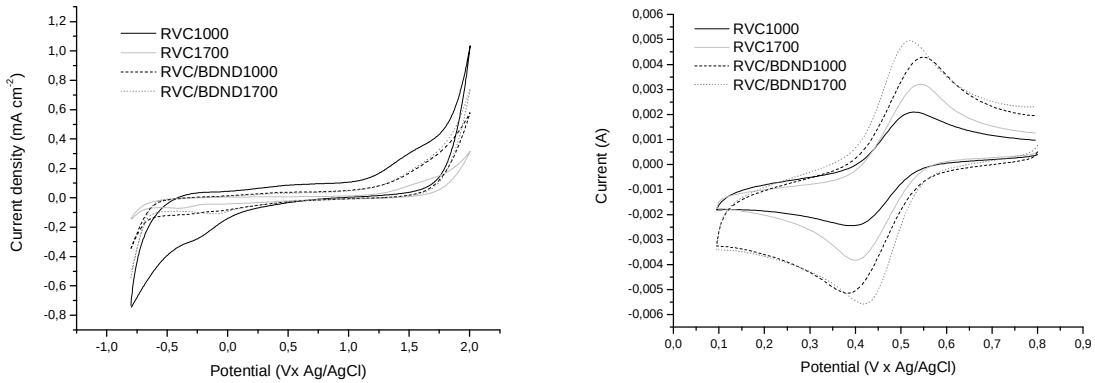

(a) (b)

Figure 4. Cyclic voltammetry i-E curves at 50 mV/s of scan rate: (a) in 0.5 mol L^{-1} H_2SO_4 solution and (b) in 1 mmol of $K_4Fe(CN)_6$ + 0.5 mol L^{-1} H_2SO_4 solution.

From Figure 5, it is possible to note the effect of BDND film through the variation of ΔE_p value. A lower variation of ΔE_p value for RVC/BDND1700 is attributed to a good conductivity for this composite, which improves the electron transfer in electrochemical experiments. This improvement was not verified for the RVC/BDND1000, also the anodic and cathodic peaks were not observed at 500 mV s^{-1} scan rates for this composite.

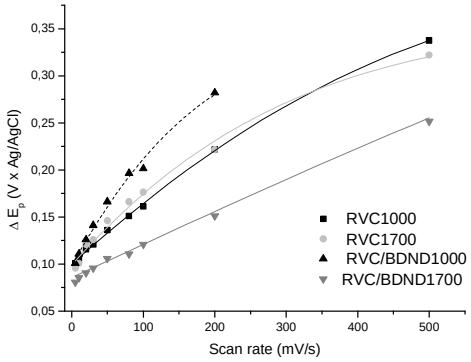

Figure 5. ΔE_p as a function of scan rate in 1 mmol of $K_4Fe(CN)_6$ + 0.5 mol L^{-1} H_2SO_4 solution.

The electrochemical response also permits to estimate the Specific Surface Area (S_s) and Specific Electrochemical Surface Area (SESA). The S_s was obtained by using the Randles-Sevcik equation:

$$S_s = Ip/v^{1/2} \times 1/\ 2{,}69.10^5\ n^{3/2}\ D_0^{1/2}\ C_0 \qquad [1]$$

Where: Ip is the anodic peak current intensity (A); v is the sweeping rate in voltammetric experiments (V s^{-1}); n is the number of electrons involved in the redox reaction; C_0 is the oxidant concentration (equal to reductor); and D_0 for the oxidant diffusivity in solution (cm^2 s^{-1}, also considered equal to reductor).

SESA value was obtained dividing the S_s by the geometric volume of the electrode (V_{el}) (Equation 2).

$$SESA = S_s / V_{el} \quad [2]$$

Table 1 shows the S_s and SESA values calculated for RVC and RVC/BDND electrodes and the number of acceptors densities in BDND films obtained by Mott-Schottky plots (MSP). It is possible to note an increase in the SESA value increasing the HTT, as a result of the electrical resistivity decrease due to a reduction in the structural defects, which is determinant to the electrochemical response. After BDND film growth, SESA increases 127% for RVC/BDND1000 and 157% for RVC/BDND1700. This result can be related to the roughness caused by the nanodiamond film which promotes a larger SESA.

Table 1. Specific Surface Area (S_s) and Specific Electrochemical Surface Area (SESA) and number of acceptors densities obtained by MSP.

Electrode	S_s (cm^2)	SESA (cm^2/cm^3)	Number of acceptors densities ($B.cm^{-3}$)
RVC1000	29.1	22.3	—
RVC1700	48.0	34.6	—
RVC/BDND1000	67.1	50.7	$3.08x10^{20}$
RVC/BDND1700	114.7	89.0	$1.29x10^{20}$

Conclusion

The RVC/BDND composites as a three dimensional electrodes were produced and characterized with success. SEM images have demonstrated a high diamond nucleation for both RVC electrodes. Raman spectra confirm the growth of nanocrystalline diamond, and heavily boron doping. RVC electrodes with different HTT and RVC/BDND composite demonstrate a quasi-reversible systems, as the *v* increasing promotes *Ip* and ΔE_p increase. The lowest ΔE_p values and the highest electrochemical area were observed for RVC/BDND1700 indicating this electrode present the highest conductivity and the fastest kinetic. Therefore, this work showed that BDND films grown on RVC are very promising for electrochemical applications.

Acknowledgments

The authors acknowledge financial support from CNPq (Process 162683/2013-8 and 303287/2013-6) and FAPESP.

References

1. N. Amini, K-F. Aguey-Zinsou and Z-X. Guo, *Carbon*, **49**(12), 3857 (2011).
2. J. Wang, *Electrochim. Acta*, **26** (12), 1721 (1981).
3. A. Dekanski, J. Stevanovic, R. Stevanovic, B. Z. Nikolic and V. M. Jovanovic, *Carbon*, **39**, 1195 (2001).

4. J. M. Friedrich, C. Ponce-de-León, G. W. Reade, F. C. Watsh, *J. Electroanal. Chem.*, **561**, 203 (2004).
5. A. F. Azevedo, M. R. Baldan and N. G. Ferreira, *Int. J. Electrochem.*, **2012**, 1 (2012).
6. O. A. Williams, M. Nesladek, M. Daenen, S. Michaelson, A. Hoffman, E. Osawa, K. Haenen and R. B. Jackman, *Diam. Relat. Mater.*, **17**, 1080 (2008).
7. O. A. Williams, *Diam. Relat. Mater.*, **20**, 621 (2011).
8. P. Morgan, *Carbon Fibers and Their Composites*, p.15, Taylor & Francis Group, New York (2005).
9. M. R. Baldan, S. C. Ramos, E. C. Almeida, A. F. Azevedo and N. G. Ferreira, *Diam. Relat. Mater.*, **17**, 1110 (2008).
10. A. V. Diniz, V. J. Trava-Airoldi, E. J. Corat and N. G. Ferreira, *Chem. Phys. Lett.*, **414**, 412 (2005).
11. S. S. Oishi, M. C. Rezende, F. D. Origo, A. J. Damião, E. C. Botelho, J. *Appl. Polym. Sci.*, **128**, 1680 (2013).
12. L. I. Medeiros, A. B. Couto, J. T. Matsushima, M. R. Baldan and N. G. Ferreira, *Thin Solid Films*, **520**, 5277 (2012).
13. M. Bernard, C. Baron and A. Deneuville, *Diam. Relat. Mater.*, **13**, 896 (2004).
14. V. Mortet, L. Zhang, M. Eckert, J. D'Haen, A. Soltani, M. Moreau, D. Troadec, E. Neyts, J-C. De Jaeger, J. Verbeeck, A. Bogaerts, G. V. Tenderloo, K. Haenen and P. Wagner, *Phys. Status Solidi A*, **209**, 1675 (2012)
15. J.P. Goss, P.R. Briddon, *Phys. Rev. B: Condens. Matter.*, **73**, 085204 (2006).
16. W. Kulisch, C. Petkov, E. Petkov, C. Popov, P. N. Gibson, M. Veres, R. Merz, B. Merz and J. P. Reithmaier, *Phys. Status Solidi A*, **209**, 1664 (2012).
17. R. Greef, R. Peat, L. M. Peter, D. Pletcher and J. Robinson, *Instrumental Methods in Electrochemistry*, Chap.6, Wiley, New York (1985).